

# A Molecular Switch Based on Potential-Induced Changes of Oxidation State

Fan Chen,<sup>†</sup> Jin He,<sup>†</sup> Colin Nuckolls,<sup>§</sup> Tucker Roberts,<sup>§</sup> Jennifer E. Klare,<sup>§</sup> and Stuart Lindsay<sup>\*,†,‡,||</sup>

*Departments of Physics and Astronomy, Chemistry and Biochemistry, and Chemistry, Columbia University, and Biodesign Institute, Arizona State University*

Received December 24, 2004

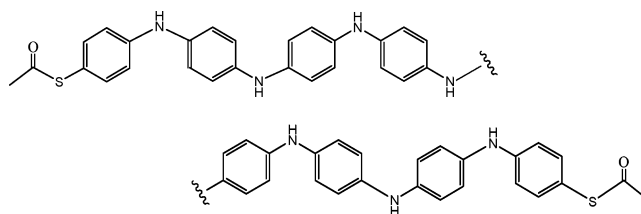
## ABSTRACT

We have measured the conductance of a hepta-aniline oligomer attached to gold electrodes held under potential control in electrolyte. It increases fifteen-fold (to  $5.3 \pm 0.4$  nS) on oxidation from the leucoemeraldine form to the emeraldine salt. The single-molecule current–voltage characteristic, linear in toluene, displays negative differential resistance in an acidic electrolyte. The negative differential resistance is accounted for by modification of the local surface potential by the applied bias. These results connect electrochemical data directly to molecular electronic behavior in a two-terminal device.

Fluctuations in the arrangement of solvent molecules and ions play a critical role in establishing the transition states that catalyze charge transfer in chemical and biological reactions.<sup>1</sup> This key ingredient has not been explored in investigations of single-molecule conductance to date. Molecules that change their oxidation state easily (redox-active molecules) have been studied<sup>2–4</sup> in cryogenic/vacuum conditions that lack the solvent fluctuations which mediate transitions between oxidation states, so there is only a rather indirect connection between electrochemistry and molecular electronics in these circumstances.<sup>5</sup> This may account for the significant discrepancies between the energy spacing of molecular levels measured in these conditions and the energy level spacing inferred from electrochemistry.<sup>2</sup> Scanning tunneling microscope (STM) studies carried out in electrolyte under potential control give results that are broadly in line with bulk electrochemistry,<sup>6,7</sup> suggesting that direct measurements of electronic conductance<sup>8</sup> need to be made in electrolyte and under potential control. This is now possible using the method of Xu and Tao<sup>9</sup> with partially insulated probes.<sup>10,11</sup> We chose oligoaniline as a first candidate for such an investigation because the parent polymer, polyaniline, undergoes dramatic changes in conductivity with changes in its oxidation state.<sup>12,13</sup> We find that the single-molecule conductance reflects the electrochemical behavior quite well. In addition, we have discovered a new phenomenon in this

nanoscale measurement: application of a modest bias across the molecule results in negative differential resistance (NDR) that is accounted for by a bias-induced change of the oxidation state of the molecule.

Measurements of single-molecule conductance were made by adsorbing a submonolayer of a thiol terminated hepta-aniline oligomer onto an Au(111) surface.<sup>14</sup> The molecule shown below was synthesized by adapting the methods of Buchwald and co-workers<sup>15</sup> to incorporate protected thiol endgroups (see Supporting Information). The gold substrate,



coated with deprotected molecules, was placed into an inert atmosphere in the sample chamber of an STM, covered with electrolyte (0.05 M H<sub>2</sub>SO<sub>4</sub>), and its surface potential,  $E_s$ , controlled with respect to a silver wire quasi-reference electrode as shown in Figure 1A.

A gold STM tip, partially coated with an insulating layer,<sup>10</sup> was held at a fixed bias,  $V_{ts}$ , with respect to the substrate and repeatedly driven into it, and then retracted. The retraction pulls a gold filament out of the surface which tends to break with some small number of molecules bridging the gap.<sup>9</sup> Further pulling results in discrete plateaus in a plot of

\* Corresponding author. E-mail: Stuart.Lindsay@asu.edu.

<sup>†</sup> Department of Physics and Astronomy, Columbia University.

<sup>‡</sup> Department of Chemistry and Biochemistry, Columbia University.

<sup>§</sup> Department of Chemistry, Columbia University.

<sup>||</sup> Biodesign Institute, Arizona State University.

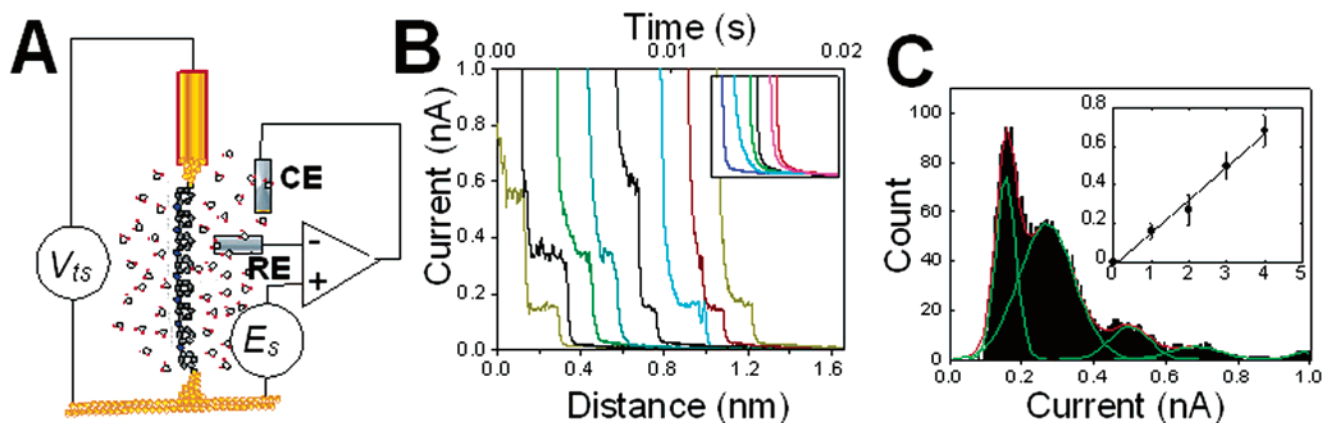


**Figure 1.** (A) Showing the gold-oligomer-gold junction with the electrode surface potential,  $E_S$ , controlled by a Pt counter electrode (CE) relative to a silver wire reference electrode (RE) and with a bias  $V_{ts}$  applied across the molecule. (B) Current vs pulling distance for the hepta-aniline oligomer in 0.05 M  $H_2SO_4$  at a potential of 0.4 V on the Ag wire scale (for  $V_{ts} = -0.2$  V). The inset shows results of the same measurement for a control experiment with no molecules present (same scales). Pulling time and distance are related via the known tip retraction speed. (C) Current distribution for the measurements in (B). The peaks correspond to 1, 2, 3, 4, and 5 molecules in the gap. The single-molecule current is found from the slope of the current vs peak number plot (inset). Peak positions were determined using Gaussian fits (green lines) to the histogram peaks (red line is sum of Gaussians). The HWHHs of these fits were used as ‘error bars’ to indicate the spread of data.

current vs time (Figure 1B) as the gold continues to yield while the molecule remains relatively undistorted.<sup>16</sup> (Current plateaus are not observed in a control experiment lacking molecules; see inset, Figure 1B.) The current plateaus occur at integer multiples of a fundamental current (peaks in Figure 1C), and the slope of a plot of the peak current vs peak number (inset, Figure 1C) yields the single-molecule current. Comparison of this approach with single-molecule connections made with gold nanoparticles<sup>8</sup> shows that that the two methods are in reasonable agreement.<sup>9,17</sup>

A cyclic voltammogram, taken in-situ in the STM sample cell (blue line, Figure 2) showed a peak at ca. 0.15 V, indicative of oxidation from the leucoemeraldine (neutral) form of the molecule to the conducting emeraldine salt. A second peak near 0.6 V reflects a further oxidation to the fully oxidized (and insulating) pernigraniline form<sup>15</sup> (see Supporting Information). The first oxidation was reversible, giving rise to the reduction peak on the return sweep. The second oxidation was not, so most experiments were limited to surface potentials below 0.5 V. The single-molecule conductance was determined as a function of  $E_S$  (red dots, Figure 2) at the small fixed bias of  $V_{ts} = -50$  mV (the tip is biased negative with respect to the substrate). The conductance is maximum when the molecule is in the emeraldine-salt form, consistent with macroscopic electrochemical measurements on polyaniline<sup>12</sup> (black dashed lines in Figure 2), falling off with increasing or decreasing potential. The falloff is more rapid than in the macroscopic case, as reported earlier for polyaniline nanowires.<sup>18</sup>

The conductance data, measured at an applied bias of 50 mV, are well fitted by a quadratic dependence on  $E_S$ :

$$G = G_{\max} - k(E_S - E_S^M)^2 \quad (1)$$

where  $G_{\max} = 5.3 \pm 0.4$  nS,  $k = 142 \pm 28$  nS/V<sup>2</sup>, and  $E_S^M = 0.36 \pm 0.01$  V. The oligomer does not become metallic

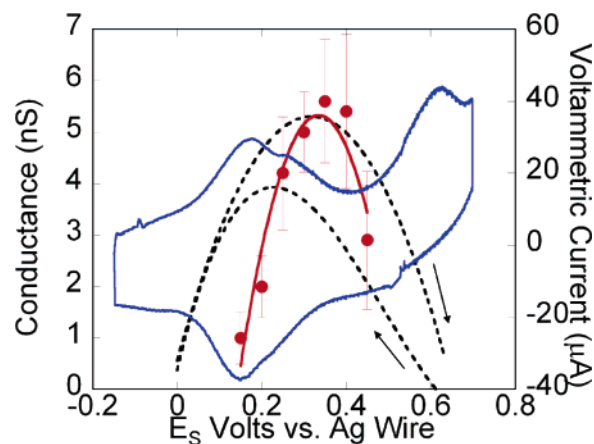


**Figure 2.** Low bias ( $V_{ts} = -50$  mV) single-molecule conductance of the aniline oligomer as a function of surface potential vs an Ag wire (red dots). The red line is a fit to a quadratic potential dependence. A cyclic voltammogram taken in-situ in the STM cell (blue line) shows the oxidation/reduction between leuco-emeraldine and emeraldine salt forms at ca. 0.15 V on this scale (see Supporting Information). The black lines show the conductivity of bulk polyaniline as measured on the same Ag wire scale by Ofer et al.<sup>12</sup> (arrows show scan direction, and the maximum is scaled to fit the single molecule peak conductance). Error bars were calculated from the width of the first peak in the current histogram to indicate the spread of data.

like the bulk polymer does.<sup>19</sup>  $G_{\max}$  (5.3 nS) is much less than  $G_0$ , the quantum of conductance ( $77 \mu S$ ), which is the magnitude of the conductivity expected in a metallic quantum wire. This difference cannot be accounted for by the limited transmission of thiol–gold contacts, because benzenedithiol has a first conductance peak at  $0.83 \mu S$ .<sup>20</sup> The metallic state in high molecular-weight polyaniline arises from a partially filled band (many levels in an energy interval comparable to  $kT$ ) in the emeraldine salt,<sup>13</sup> but level-spacing is likely to be much larger in this short oligomer.

The current–voltage characteristic of the neutral (leucoemeraldine) form of the molecule was determined by carrying

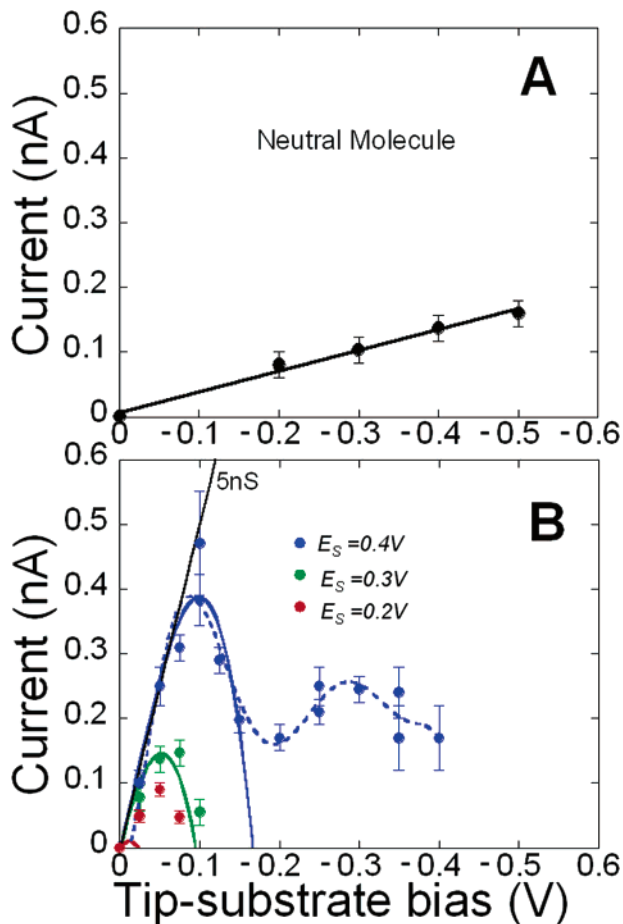


**Figure 3.** Single-molecule current–voltage data (average of ca. 1000 molecules for each point) for (A) the hepta-aniline oligomer in toluene (black dots) and (B) under potential control in 0.05 M  $\text{H}_2\text{SO}_4$  (blue dots,  $E_S = 0.4$  V; green dots,  $E_S = 0.3$  V, and red dots,  $E_S = 0.2$  V). Currents calculated using eq 2 with  $\alpha = 1.4$  and the measured potential dependence of conductivity are shown by the solid blue line ( $E_S = 0.4$  V), green line ( $E_S = 0.3$  V), and a red line close to the origin ( $E_S = 0.2$  V). All potentials are vs an Ag. wire. Error bars are widths of first peak in current histogram.

out a series of measurements at different biases with the molecule immersed in toluene. This solvent was chosen to impede oxidation or reduction of the molecule by the applied bias ( $V_{\text{ts}}$ ) so that the molecule remained unchanged as the bias was varied. The resultant characteristic (black dots, Figure 3A) is linear (Ohmic), yielding a conductance of  $0.32 \pm 0.03$  nS. The magnitude of the conductivity and the linear response in this bias range are generally consistent with transport by ballistic tunneling.<sup>8,9,21</sup>

A completely different response is observed when the same molecule is held under potential control in electrolyte. Data for  $E_S = 0.4$  V are shown by the blue dots in Figure 3B. The low bias conductance is 5 nS, as expected (Figure 2), but when the applied bias becomes more negative than ca.  $-0.1$  V, the current falls significantly, and then peaks slightly again near  $V_{\text{ts}} = -0.3$  V, becoming similar to the current through the neutral molecule by  $-0.4$  V. (Experiments were limited to negative tip biases because of the nonreversibility of the second oxidation which occurs at more positive bias.) NDR has been reported in other molecules<sup>22–24</sup> but at much

higher bias, and without electrochemical potential control of the electrode surface.

NDR is to be expected if the applied bias alters the local surface potential enough to change the oxidation state of the molecule, a possibility that can be tested with a simple model. Using the measured dependence of the conductance on surface potential (Figure 2 and eq 1) we can write

$$i = GV_{\text{ts}} = (G_{\text{max}} - k(E_S - E_S^M - \alpha V_{\text{ts}})^2)V_{\text{ts}} \quad (2)$$

where  $\alpha$  quantifies the relative influence of the tip–substrate bias on the surface potential. The solid blue line in Figure 3B shows a fit of eq 2 to the data near the current peak with  $\alpha = 1.4$ . The model was further tested by using the same value of  $\alpha$  to predict the currents at  $E_S = 0.3$  V (green line) and  $0.2$  V (red line near the origin). Data taken at  $E_S = 0.3$  V (green dots) are in good agreement with the prediction. Data taken at  $E_S = 0.2$  V (red dots) agree less well but trend in the right direction. Thus this simple model captures many of the features of the observed NDR, though a microscopic model is required to understand the details (including the observation that  $\alpha > 1$ , implying that the applied bias influences the oxidation state of the molecule more than the surface potential of the substrate). It is interesting to note that NDR is not observed in micron-<sup>12</sup> or nanoscale<sup>18</sup> polyaniline devices. Thus the strong influence of the applied bias arises either from the small scale of the single-molecule junction, or the covalent attachment of the molecules to the metal electrodes, or from a combination of both factors.

The results presented thus far are based on averages of a large number of single-molecule measurements, so they do not reveal details of the heterogeneity of the individual molecular environments. To gain information that goes beyond the current distributions (e.g., Figure 1C), the STM tip was moved in and out of the surface slowly, and stopped when a current plateau close to a measured average was observed. Then the tip–substrate bias (Figure 4A) or the substrate potential (Figure 4B) was swept and current recorded for those cases where the molecule appeared to have remained in the gap. The data taken by sweeping the tip bias showed evidence of the NDR peak (Figure 4A), but the response of each molecule was quite different. A significant fraction of the complex features recorded in the upward sweep are retraced in the downward sweep (Figure 4A) so these complex responses are not noise, but reflect aspects of the microenvironments of each of the molecules that remain constant over the time of the sweep (ca. 1 s). The current vs potential sweeps (at a fixed  $V_{\text{ts}}$ , Figure 4B) track the averaged data (Figure 2) but show sharp jumps, as reported for polyaniline nanowires.<sup>18,25</sup> These jumps are often similar in magnitude to the current through a single molecule (bars on Figs 4B and C), so they may reflect fluctuations of the thiol–gold/gold–gold bonds as observed for alkanethiols attached to Au(111).<sup>26</sup>

The results presented here demonstrate the critical role of environment in electron transport in molecules and illustrate how the electrochemical properties of a molecule can be related to its molecular electronic behavior if conductance

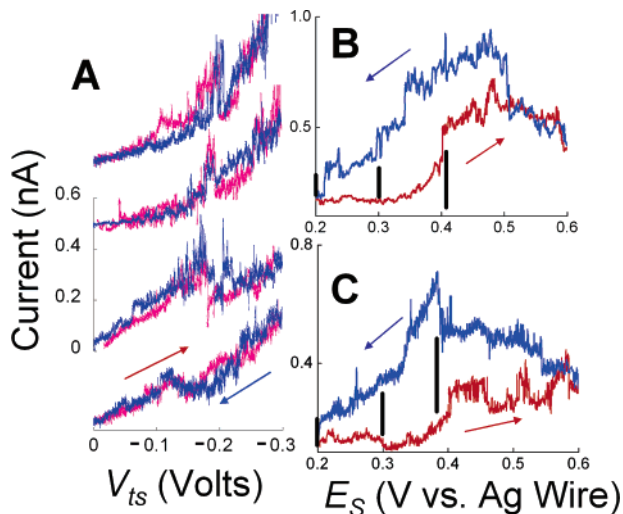


**Figure 4.** (A) *Spatial inhomogeneity*: measurements on single molecules trapped in a break-junction at  $E_S = 0.4$  V show NDR peaks with “noise” that is frequently retraced on the sweep back (scan up is red, scan down is blue, and curves are arbitrarily displaced vertically for clarity). (B) and (C) *Temporal fluctuations*: Current vs potential plots ( $V_{ts} = 50$  mV) follows the average behavior (Figure 2) but show the ‘telegraph’ switching noise reported earlier for nanoscale polyaniline wires.<sup>18,25</sup> Curves are for multiple molecules trapped in the gap, and the scale of the fluctuations compared to the measured single molecule currents (shown at 0.2, 0.3, and 0.4 V by the black bars) suggests that they arise from spontaneous contact breaking.

data are obtained under potential control. Bias-induced NDR might prove valuable as a basis for two-terminal nanoscale devices if enough molecules are incorporated into the device to overcome the strong influence of single-molecule fluctuations.

**Acknowledgment.** This work was supported by the National Science Foundation through NIRT (ECS01101175) and NSEC (CHE-0117752) awards and the New York State Office of Science, Technology, and Academic Research. We thank Nongjian Tao, Jean-Luc Bredas, and Mark Ratner for useful discussions and Iris Visoly-Fisher and Brian Ashcroft for help in the lab.

**Supporting Information Available:** Sample preparation, preparation and characterization of monolayers, cyclic voltammetry. This material is available free of charge via the Internet at <http://pubs.acs.org>.

## References

- (1) Marcus, R. A. *J. Phys. Chem.* **1965**, *43*, 679–701.
- (2) Kubatkin, S.; Danilov, A.; Hjort, M.; Cornil, J.; Bredas, J.-L.; Stuhr-Hansen, N.; Hedegard, P.; Bjornholm, T. *Nature* **2003**, *425*, 698–701.
- (3) Liang, W.; Shores, M. P.; Bockrath, M.; Long, J. R.; Park, H. *Nature* **2002**, *417*, 725–728.
- (4) Park, J.; Pasupathy, A. N.; Goldsmith, J. I.; Chang, C.; Yaish, Y.; Petta, J. R.; Rinkoski, M.; Sethna, J. P.; Abruna, H. D.; McEuen, P. L.; Ralph, D. C. *Nature* **2002**, *417*, 722–725.
- (5) Mazur, U.; Hipps, K. W. *J. Phys. Chem.* **1995**, *99*, 6684–6688.
- (6) Tao, N. *Phys. Rev. Lett.* **1996**, *76*, 4066–4069.
- (7) Gittins, D. I.; Bethell, D.; Schiffrin, D. J.; Nichols, R. J. *Nature* **2000**, *408*, 67–69.
- (8) Cui, X. D.; Primak, A.; Zarate, X.; Tomfohr, J.; Sankey, O. F.; Moore, A. L.; Moore, T. A.; Gust, D.; G., H.; Lindsay, S. M. *Science* **2001**, *294*, 571–574.
- (9) Xu, B.; Tao, N. *J. Science* **2003**, *301*, 1221–1223.
- (10) Nagahara, L. A.; Thundat, T.; Lindsay, S. M. *Rev. Sci. Instrum.* **1989**, *60*, 3128–3130.
- (11) Xu, B.; Zhang, P. M.; Li, X. L.; Tao, N. *Nano Lett.* **2004**, *4*, 1105–1108.
- (12) Ofer, D.; Crooks, R. M.; Wrighton, M. S. *J. Am. Chem. Soc.* **1990**, *112*, 7869–7879.
- (13) Bredas, J. L. The Polyanilines: Illustration of the Interconnection Between Chemical Structure, Geometric Structure, and Electronic Structure in Conjugated Polymers. In *Conjugated Polymers and Related Materials: Proceedings of the 1991 Nobel Symposium in Chemistry*; Salaneck, W. R., Lundström, I., Rånby, B., Eds.; Oxford University Press: Oxford, 1993; Vol. NS81, pp 187–221.
- (14) DeRose, J. A.; Thundat, T.; Nagahara, L. A.; Lindsay, S. M. *Surf. Sci.* **1991**, *256*, 102–108.
- (15) Sadighi, J. P.; Singer, R. A.; Buchwald, S. L. *J. Am. Chem. Soc.* **1998**, *120*, 4960–4976.
- (16) Xu, B.; Xiao, X.; Tao, N. *J. Am. Chem. Soc.* **2003**, *125*, 16164–16165.
- (17) Tomfohr, J.; Ramachandran, G.; Sankey, O. F.; Lindsay, S. M., Making contacts to single molecules: Are we nearly there yet? In *Introducing Molecular Electronics*; Fagas, G., Richter, K., Eds.; Springer: Berlin, 2005.
- (18) He, H.; Zhu, X. J. S.; Tao, N. *J. Appl. Phys.* **2001**, *78*, 811–813.
- (19) Prigodin, V. N.; Epstein, A. J. *Synth. Met.* **2001**, *125*, 43–53.
- (20) Xiao, X.; Xu, B. Q.; Tao, N. *Nano Lett.* **2004**, *4*, 267–271.
- (21) Tomfohr, J. K.; Sankey, O. F. *J. Chem. Phys.* **2004**, *120*, 1542–1554.
- (22) Chen, J.; Reed, M. A.; Rawlett, A. M.; Tour, J. M. *Science* **1999**, *286*, 1550–1552.
- (23) Gorman, C. B.; Carroll, R. L.; Fuieler, R. R. *Langmuir* **2001**, *17*, 6923–6930.
- (24) Guisinger, N. P.; Greene, M. E.; Basu, R.; Baluch, A. S.; Hersam, M. C. *Nano Lett.* **2004**, *4*, 55–59.
- (25) He, H. X.; Li, X. L.; Tao, N. J.; Nagahara, L. A.; Amlani, I.; Tsui, R. *Phys. Rev. B* **2003**, *68*, 045302–8.
- (26) Ramachandran, G. K.; Hopson, T. J.; Rawlett, A. M.; Nagahara, L. A.; Primak, A.; Lindsay, S. M. *Science* **2003**, *300*, 1413–1415.

NL0478474